

International Conference on Space Optics—ICSO 2014

La Caleta, Tenerife, Canary Islands

7–10 October 2014

Edited by Zoran Sodnik, Bruno Cugny, and Nikos Karafolas



NEuclid: a long-range tilt-immune homodyne interferometer

M. J. Bradshaw

C. C. Speake



International Conference on Space Optics — ICSO 2014, edited by Zoran Sodnik, Nikos Karafolas,
Bruno Cugny, Proc. of SPIE Vol. 10563, 1056340 · © 2014 ESA and CNES
CCC code: 0277-786X/17/\$18 · doi: 10.1117/12.2304248

nEUCLID – A LONG-RANGE TILT-IMMUNE HOMODYNE INTERFEROMETER

M.J. Bradshaw¹ and C. C. Speake²
mjb@star.sr.bham.ac.uk¹, c.c.speake@bham.ac.uk²

^{1,2}*School of Physics and Astronomy, University of Birmingham, Birmingham, B15 2TT, UK,*

I. INTRODUCTION:

The new Easy to Use Compact Laser Interferometric Device (nEUCLID) is a polarisation-based homodyne interferometer with substantially unequal arms that is tolerant to target mirror tilt. The design has no active components, uses standard optical components of 25 mm diameter, has a working distance of 706 mm and a reference arm-length of 21 mm. nEUCLID optics have a footprint of 210 x 190 x 180 mm, and has a tolerance to target mirror tilt of ± 0.5 degrees, made possible by a novel new retro-reflector design [1].

nEUCLID was built to a set of specifications laid down by Airbus Defence and Space, who required a low-mass, low-power device to measure displacement with nanometre accuracy for space applications. At the University of Birmingham we have previously built a smaller, more compact tilt-insensitive homodyne interferometer – the EUCLID [2, 3, 4] – which has a working distance of 6 mm, a working range of ± 3 mm, and a tilt range of $\pm 1^\circ$ [2]. We created a new optical design to allow a much larger working distance to be achieved (as discussed in Section II) and used this in a new interferometer – the nEUCLID.

Section II describes the interferometer in detail; how nEUCLID is tilt insensitive, and the optical configuration. Section III states the design specifications from Airbus Defence and Space and the components used in the final design. The output interference pattern from nEUCLID, and how it has been corrected with a meniscus lens, is also discussed. In Section IV we discuss the results demonstrating the tilt immunity range, and the sensitivity of the device. Section V describes several potential applications of nEUCLID, and Section VI draws together our conclusions.

II. DESCRIPTION OF THE INTERFEROMETER:

A. Mirror Tilt Immunity

We have developed a simple novel optical design for a cat's eye retro-reflector, developed specifically for a tilt insensitive interferometer with substantially unequal arms [1]. The new optical design behaves effectively as an ideal cat's eye, but is referred to as a 'quasi-cat's eye'. As can be seen in Fig. 1, we have inverted the lenses in the quasi cat's eye, compared with previous conventional designs [3]. Comparing the performance of the new design with a conventional cat's eye optical configuration, it was shown that only the quasi cat's eye is able to achieve the long working distance with unequal arm lengths required for this application (for more detail, see [1]).

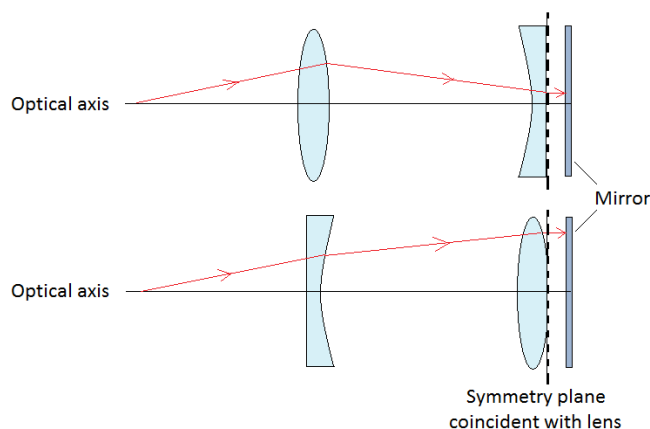


Fig. 1. Top: Diagram of a conventional cat's eye. Bottom: The quasi cat's eye, as used in nEUCLID.

The new cat's eye has an extra term, δ , producing additional focusing of the beam. It was calculated that the δ term produces negligible errors in the optical path measurement [1]; however, it also causes an increase in radius of curvature, thus the interference pattern to be created of closely-spaced circular fringes. These can be very difficult to resolve, and cause the photodiode to average across the pattern, giving a low overall visibility. To solve this problem, we added a meniscus lens to the reference arm. This enlarged the radius of curvature of the reference beam to approximately that of the target beam, creating a much broader, clearer interference pattern (see Figs. 3 and 4). Section III contains more detail on how the δ term affects the output interference pattern.

This optical design is not limited to a target arm length of only 706 mm; theoretically, the cat's eye design allows interferometers to be created with target arm lengths of several metres. However, as specified in Table 1, we were initially aimed at creating a prototype that would fit on a 1 m display rail.

B. Layout of the interferometer

Fig. 3 shows a schematic diagram of the interferometer. Upon entry to the set-up, the beam is attenuated by a polariser. This attenuation prevents optical feedback, which causes laser instability. Once the beam has left the collimator it passes through a polarising beam splitter (PBS 1). The laser has been orientated to ensure the beam is only of one plane of polarisation (p-), thus all the intensity passes through PBS 1. The beam passes through a non-polarising beam splitter (NPBS), where it loses roughly 50% intensity. It passes through a half-wave plate (HWP) orientated to 22.5° , which rotates the plane of polarisation of the beam by 45° , which, upon having entered PBS 2, sends the p-polarisation to the reference arm and the s-polarisation beam to the target arm.

The target arm beam passes through a quarter wave plate (QWP) and on towards the target mirror. Having reflected off the target mirror, the target beam passes back through the QWP, causing it to now pass through PBS 2 as p-polarisation, and on to the cat's eye lenses. The beam travels through the concave lens, followed by the convex lens, reflects off the mirror and returns back through the two lenses and through PBS 2 and the QWP again, to reflect off the target mirror. The target beam passes back through the QWP one more time, causing it to now reflect off PBS 2 (as s-polarisation) and back towards the laser. Here it recombines with the reference beam.

In the meantime, the reference beam has travelled through a polariser, which adjusts the intensity to create the best visibility at the photodiodes. The reference beam travels through the meniscus lens, to reflect off the reference mirror and return back through the polariser, and through PBS 2. Here it recombines with the target beam. The target beam has now accrued extra phase from the extra path length travelled.

With the two beams recombined, the beam passes back through the HWP and is split in half by the NPBS. Half the intensity travels onwards, and the other half is reflected through a second QWP and a third PBS. These two components act to separate the two polarisation components, with the QWP introducing a phase shift of $\pi/2$ between them. Each beam then passes on to a photodiode. The beam that travelled on from the NPBS is reflected by PBS 1 and passes onto a third photodiode.

The three photodiode signals are used to calculate the displacement of the target mirror, via the interference pattern produced. For more detail on this method, please refer to [4].

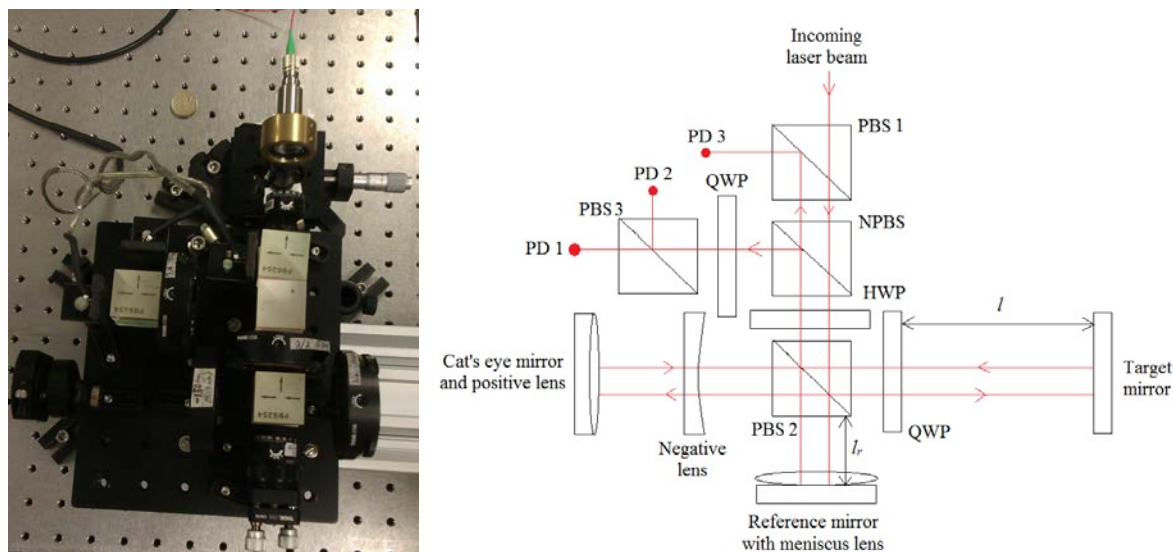


Fig. 2. Left: Photograph of the nEUCLID optics in the laboratory. Right: Corresponding schematic diagram of the set-up, where l is the length of the target arm, and l_r the reference arm.

III. IMPLEMENTATION:

A. Design Specification:

For space applications, a set of requirements was decided by Airbus Defence and Space. This meant we were constrained by these measurements when we built nEUCLID. The requirements and current prototype specifications are shown in Table 1 (including the electronics box, but discounting the aluminium rail mount shown in Fig. 2, which is purely for display purposes).

	Specification	Current Design
Dimensions (mm)	~ 230 x 220 x 200	210 x 190 x 180
Working Distance (mm)	~ 1000	706
Mass (kg)	< 3	~ 2.0
Power (W)	< 5	~ 1.8

Table 1. The specifications and current design of nEUCLID.

B. Modelling the Output Interference Pattern:

The resulting interference pattern from nEUCLID was modelled to ensure the best possible visibility on the photodiodes. As explained in Section II, the meniscus lens was placed in the reference arm to counteract the effect of the δ term on the output beam. This ensured the reference and target beams were similar in radius of curvature, thus creating a better visibility (for more detail on the meniscus lens and its effects, refer to [1]).

The visibility of an interference pattern is defined as

$$V = \frac{I_{\max} + I_{\min}}{I_{\max} - I_{\min}} \quad (1)$$

where I_{\max} is the maximum intensity value of the interference pattern, and I_{\min} is the minimum intensity value.

A visibility of unity would be the best interference pattern possible. Figures 3 and 4 demonstrate what is predicted from nEUCLID and what we have actually observed.

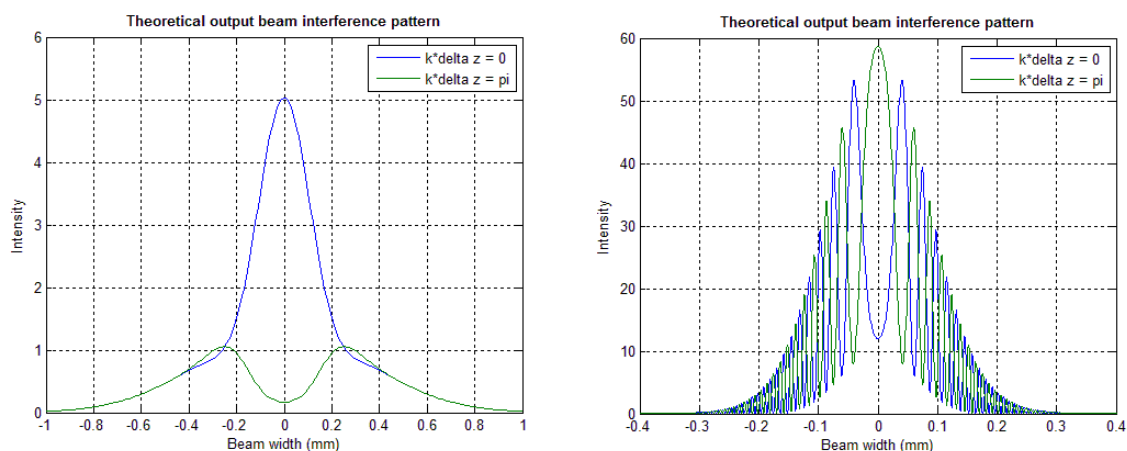


Fig. 3. Left: The predicted interference pattern with meniscus lens in reference arm. Right: Predicted interference pattern without meniscus lens in reference arm. (A width of 2.0 mm has been specified as this is the diameter of the photodiodes in the interferometer. The scale is smaller in the right-hand plot due to the tight fringe pattern).

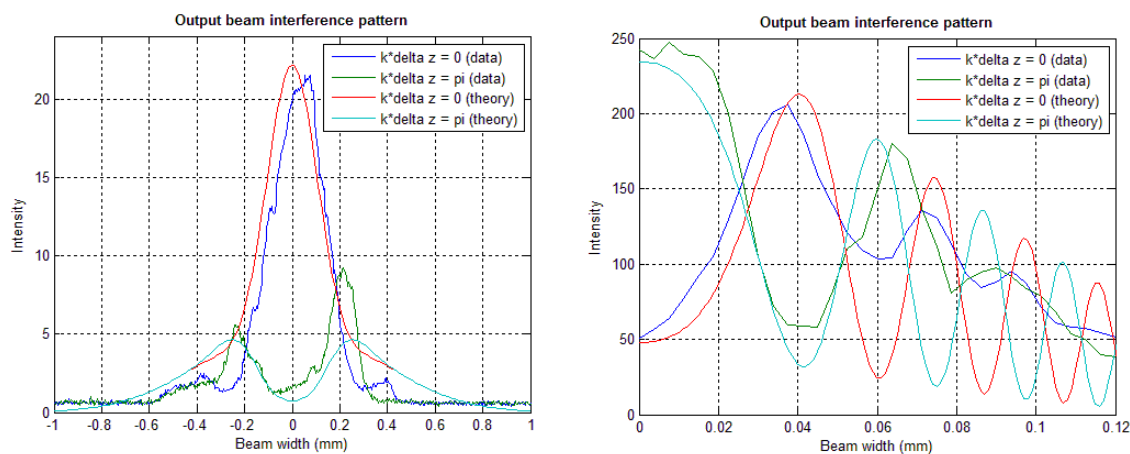


Fig. 4. Left: The theoretical and real interference pattern with the meniscus lens. Right: A close-up of the interference pattern without the meniscus lens. Again, a close-up was necessary to easily distinguish individual fringes in such a tight pattern.

With the meniscus lens, the visibility of the real data is 0.48, compared to 0.68 from the theoretical data. Without the meniscus lens, the visibility over this range (0.12 mm) for the real data is only 0.24, and 0.29 from the theoretical data.

C. Component Specification:

A DFB fibre-fed laser is used, wavelength 1550 nm, connected from the purpose-built electronics box [5] to an FC/APC collimating lens via a polarising-maintaining, single-mode patch cord fibre. The polarisers on the input of the laser and in the reference arm are both made from material equivalent to Polaroid HR. The polarising and non-polarising beam splitters are 25.4 mm³ and IR-coated; the PBS made of N-SF1, and the NPBS of N-BK7. The three mirrors are 25.4 mm diameter protected aluminium, with a surface flatness of $\lambda/10$. The quarter-wave and half-wave plates are 25 mm in diameter, made of mica. The concave cat's eye lens is 50.8 mm in diameter, the convex cat's eye lens is 25.4 mm in diameter, and both are made from N-BK-7. All

the optics are mounted on non-magnetic 303 series stainless steel posts on an anodised aluminium breadboard, attached to an aluminium rail. The photodiodes used are InGaAs and are 2 mm diameter.

Fig. 5 shows nEUCLID in its final configuration, as it is used in the laboratory. It is mounted on an aluminium rail of length 1 m, to allow the target mirror (on the right-hand side of image) to be moved easily towards/back from the interferometer. The electronics box (silver) [5] records the photodiode data and calculates the displacement, which is displayed on the laptop.



Fig. 5. Photograph of nEUCLID in the laboratory.

IV. RESULTS

Fig. 6 shows the visibility of the interference pattern at the photodiodes over a range of tilt of the target mirror. The visibility averages to 0.65, which is highly visible. We can also see the tilt range achievable by nEUCLID: $1^\circ (\pm 0.5^\circ)$, with the visibility decreasing as the beam moves off the optics.

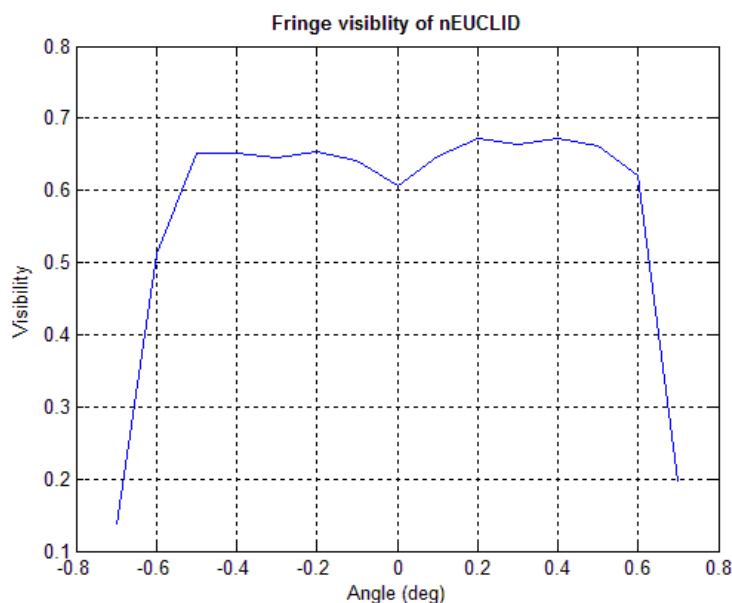


Fig. 6. Example of the fringe visibility measured by the photodiodes in nEUCLID.

We are currently investigating the working range of nEUCLID. Fig. 6 shows the visibility for only one position of the target mirror – the ‘sweet plane’, where the greatest visibility is achievable (see [1] for more detail). As

the target mirror is moved away from the sweet plane, we expect the visibility to linearly decrease, as it does in the EUCLID interferometer [2, 3]. These results will be presented in a later paper, currently in preparation [6].

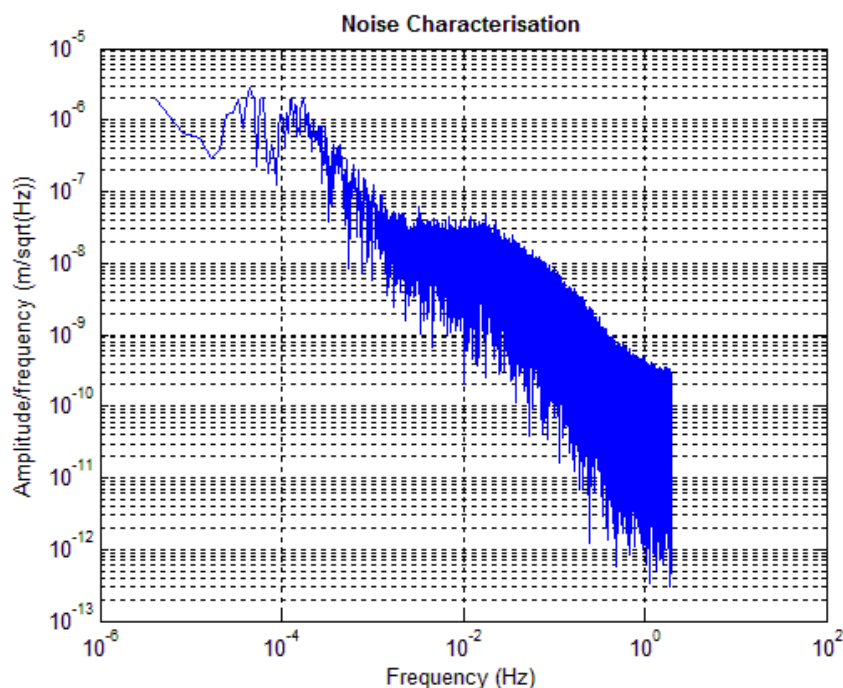


Fig. 7. Plot of nEUCLID sensitivity, taken in air in the laboratory.

Fig. 7 shows the sensitivity of nEUCLID in air over a period of 65 hours. At 1Hz, nEUCLID has a sensitivity of 445 pm per $\text{Hz}^{-1/2}$. At lower frequencies (approximately 10^{-4} Hz), we currently see oscillations of amplitude 0.06 μm that have a period of almost two hours. We suppose this is due to the laser system, and are investigating it further with the intent to remove it entirely from the system.

V. POTENTIAL APPLICATIONS:

We are currently in discussion with Airbus Defence and Space about several potential applications for nEUCLID. These include:

- Antenna metrology
- Deployable structures
- Adaptive optics
- Formation flying missions

The most promising of these is the use of nEUCLID for monitoring the potential distortion of antenna shape for telecommunication satellites as they pass in/out of eclipse. Monitoring antenna distortion is also applicable for Earth observation (EO) missions. Fig. 8 shows one of the applications discussed with Airbus Defence and Space; monitoring the position of the phase centres on the antenna arms of a potential EO mission.

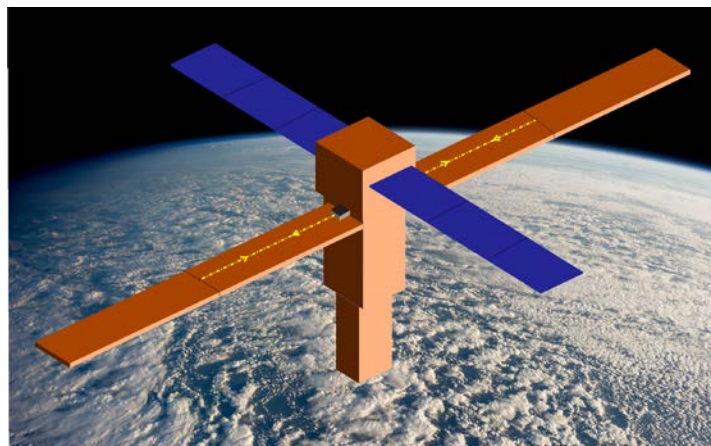


Fig. 8. Sketch of Wavemill, a Phase 0 Earth observation mission, with nEUCLID marked on the diagram close to the satellite body. The yellow dotted lines indicate the measurement beam.

VI. CONCLUSIONS:

We have built a long-range tilt-insensitive homodyne interferometer, with a novel new cat's eye retro-reflector design. It has a target arm length of 706 mm, with the capacity to extend this to several metres with further interferometer designs. The working range is being investigated, but at the sweet plane (position of best interference pattern visibility) nEUCLID has a tilt range of $\pm 0.5^\circ$. This range is limited by the diameter of the optics. The interferometer has a sensitivity of 445 pm per $\text{Hz}^{-1/2}$ at 1 Hz. We are discussing several applications for nEUCLID with Airbus Defence and Space, focusing on antenna metrology.

ACKNOWLEDGEMENTS:

This work was funded by STFC and Airbus Defence and Space Ltd. We would like to thank Dr Christian Trenkel (Airbus Defence and Space) for his input and expertise regarding space technology and applications. We would also like to thank John Bryant and David Hoyland for their assistance with the software and electronics for this project. MJB is grateful to the Royal Astronomical Society and the Institute of Physics for the travel funding awarded to her to attend this conference.

REFERENCES

- [1] C. C. Speake, M. J. Bradshaw, "A novel quasi-cat's eye for improved mirror-tilt-free interferometry", *Applied Optics*, 2014, in preparation
- [2] S. M. Aston, "Optical Read-out Techniques for the Control of Test-masses in Gravitational Wave Observatories", University of Birmingham, 2011
- [3] F. E. Peña Arellano, C. C. Speake, "Mirror Tilt Immunity Interferometry with a Cat's Eye Retroreflector", *Applied Optics*, 1:50(7): 981-91, 2011
- [4] C. C. Speake, S. M. Aston, "An Interferometric Sensor for Satellite Drag-Free Control," in *Classical and Quantum Gravity*, vol. 22. Institute of Physics Publishing Ltd, UK, pp. 269 - 277, 2005.
- [5] C. C. Speake, D. Hoyland, J. Bryant, "EUCLID User Guide – Issue 2.9", University of Birmingham, 2014
- [6] M. J. Bradshaw, C. C. Speake, 2014, in preparation